Grout-Filled Pipe Splices for Precast Concrete Construction

Amin Einea
Ph.D., P.E., S.E.
Research Assistant Professor
Center for Infrastructure Research
University of Nebraska-Lincoln
Omaha, Nebraska

Takashi Yamane
Chief Engineer
Kyokuto Corporation
Presently Graduate Assistant
Civil Engineering Department
University of Nebraska-Lincoln
Omaha, Nebraska

Maher K. Tadros
Ph.D., P.E.
Cheryl Prewett Professor of
Civil Engineering and
Director,Center for
Infrastructure Research
University of Nebraska-Lincoln
Omaha, Nebraska

The effect of confining entire members or parts of members, such as beams and columns, is known to strengthen the bond between the concrete and reinforcement. In this paper, the effect of confining the grout that surrounds isolated, single reinforcing bars on the bond strength between the bar and the grout is investigated. Grout-filled steel pipe splices with different parameters and geometrical design were prepared and loaded in axial tension until failure. The test specimens are described and the test results are presented, with discussion and analysis in light of existing theory. The experimental results show that a generic and inexpensive reinforcing bar splice for field connection of precast concrete members can be achieved using grout-filled standard steel pipe.

Confining concrete is known to increase the effective bond strength between reinforcing bars and the surrounding concrete. This behavior has been studied by several researchers through experimental and analytical studies of axially or flexurally loaded specimens. Those studies, however, concentrated on confining entire members, or large regions of members, rather than confining the concrete surrounding individual bars.

Grout filled splices have been in use for the past two decades in North America, Europe, and Japan to connect precast concrete members. Figs. 1 and 2 give examples of common applications. Sleeves are inserted during the fabrication process on one side of the connected member. Rein-

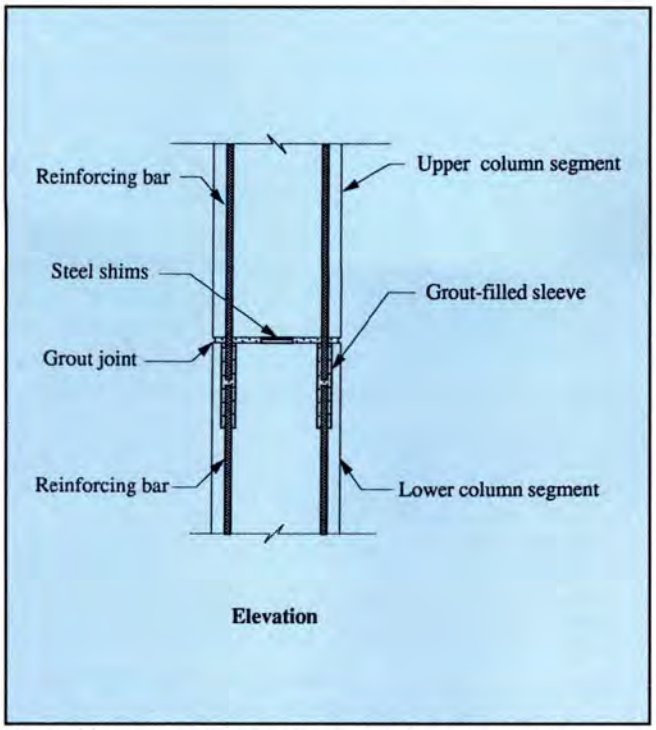

Fig. 1. Moment resistant column-to-column connection.

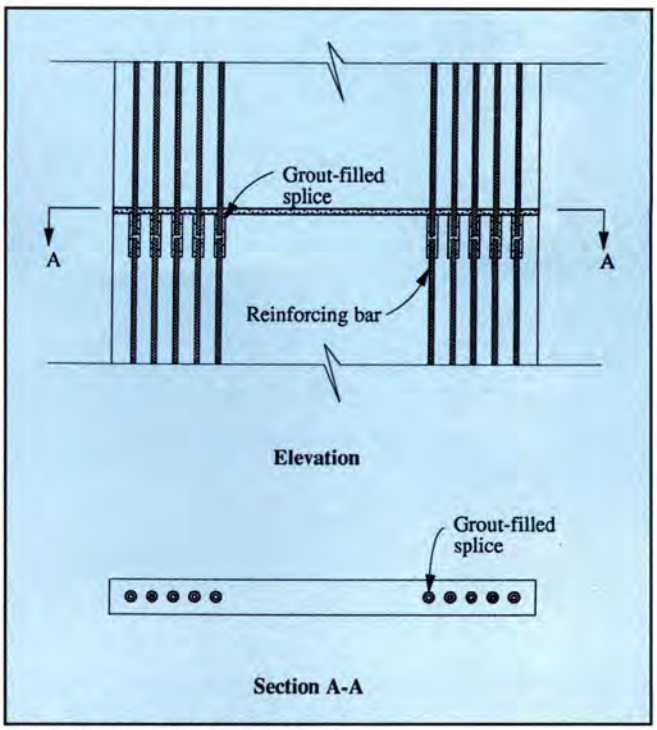

Fig. 2. Connection of wall panels.

forcing bars project from the other side. In the field, the two sides are fitted together by inserting the projecting bars into the sleeves. The air space between the bars and the sleeve is then filled with grout, usually by pumping fluid grout into the sleeve.

Sometimes, it is possible to place grout in the sleeve before the bars are inserted in order to avoid the extra step of grout pumping. These splices rely primarily on grout strength and confinement to improve bond stress and, thus, result in a short development length of the spliced bars within the grout-filled hardware. The sleeves available on the market are proprietary products and little information has been published on the relationship between grout confinement and bar strength development.

The objective of the research presented in this paper is two-fold:

1. To evaluate the bond strength of reinforcing bars as a function of grout compressive strength and the level of confinement.

2. To investigate the feasibility of utilizing a generic grout-filled reinforcing bar splice. The benefit of this system is a non-proprietary splice that is inexpensive and has satisfactory performance for use in precast concrete construction.

To carry out the objectives of this investigation, 14 specimens were load tested in tension. Specimens with various parameters and configurations were prepared and loaded in axial tension to study their behavior with variables such as level of confinement, embedment or lap lengths, compressive strength of grout, and other parameters. Confinement was provided by commercially available steel pipes.

This paper summarizes existing research, describes the test specimens, presents the test results, and discusses the results in light of existing bond theories.

PREVIOUS RESEARCH

The general concept of the effect of concrete confinement on concrete behavior and the effective bond strength between reinforcing bars and the surrounding concrete has been studied by several researchers. Most available literature, however, concentrates on the concept as it applies to entire reinforced concrete members or major portions of the members in which more than a single bar is confined inside one confining system.

Untrauer and Henry (1965) found that the bond strength between steel and concrete increases linearly with normal pressure.[1] They applied normal pressure to two parallel faces of their specimens concurrently with the pull-out forces. They derived an equation that represents the relationship between the compressive strength of concrete, normal pressure, and reinforcing bond strength.

The slip of a bar in unconfined concrete has been measured by Nilson (1972).[2] He derived a relationship between bond stress and bar slip in reinforced concrete. An equation to calculate bond stress from the slope of the stress-strain curve of the reinforcing bar was developed. In addition, a method to determine the slip from the displacement function by numerical integration of the strain was presented.

Testing and analysis of bond failure of deformed bars, based on the longitudinal splitting of the surrounding concrete effect, was performed by Losberg and Olssen (1979).[3] Their report includes a study of deformation and splitting forces.

Yankelevsky (1985) proposed an analytical method to define the relationship between axial stress in the bar and bond strength.[4] His mathematical derivation, with the bar tensile force as a variable, leads to a second order differential equation. The solution of the equation agreed with his experimental

Table 1. Properties of steel pipes (ASTM Specification A500 Grade A).

Nominal diameter (in.)	Outside diameter (in.)	Inside diameter (in.)	Wall thickness (in.)	Cross-sectional area (in.)	F_y/F_u (ksi)
3	3.500	3.068	0.216	2.23	33.5/55.2
2	2.375	2.067	0.154	1.07	
1½	1.900	1.610	0.145	0.799	

Note: 1 in. = 25.4 mm; 1 ksi = 6.89 MPa..

Table 2. Properties of specimens.

Type of specimen	Specimen number	L_d (in.)	Main bar size	Lapping bar size	Pipe diameter (in.)	Figure number
Type 1 lapping bar	1	10	No. 9 (29 mm)	No. 9 (29 mm)	3	1a
	2	8				
	3	6				
Type 2 lapping bar	1	8	No. 6 (19 mm)	4 – No. 3 (4 – 10 mm)	2	1b
	2	7				
	3	6				
Type 3 steel ring	1	7	No. 6 (19 mm)	—	2	1c
	2	6				
	3	5				
	4	7	No. 6 (19 mm)	—	2	
	5	6				
	6	5				
Type 4 steel plate	1	5	No. 5 (16 mm)	—	1½	1d
	2	6	No. 6 (19 mm)			

Note: 1 in. = 25.4 mm.

results at steel stresses lower than about 23 ksi (160 MPa).

Soroushian and Choi (1989) investigated the local bond stress behavior of deformed bars in confined concrete.[5] They concluded that the bond strength decreased linearly as the bar diameter increased. The characteristic bond slip values (e.g., those corresponding to the peak bond strength), however, are not consistently influenced by the variations in bar diameter.

Soroushian et al. (1991) reported the results of a bar pull-out testing program.[6] They found that the ultimate bond strength is directly proportional to the square root of the compressive strength of concrete. The relationship between the local bond stress and bar slippage, however, is not highly affected by the compressive strength of concrete.

Hayashi et al. (1993) found a relationship between the maximum local bond stress and the slip of a bar in a grout-filled deformed steel sleeve.[7] Their results indicate that bond stress increases linearly with grout strength at the non-yielded portion of the bars while it is constant at the yielded portion of the bars regardless of the grout strength.

Nomura et al. (1993) tested bar splice specimens with capped sleeves filled with a high-expansion grout.[8] Some of the tested specimens resulted in bar failure rather than bond failure.

Adajar et al. (1993) performed an experimental bar splicing investigation using a combination of lapping bars and confining spirals.[9] Main bars were spliced in grout-filled ducts that were surrounded by steel lapping bars and spiral. They concluded that the ultimate strength of the splices used in their investigation is equal to the tensile strength of the spliced bar when the lapping distance equals or exceeds 25 times the bar diameter.

TEST PROGRAM

To fulfill the objectives of this research, a test program was carried out on specimens with various sizes and details. The main reason for this variety in specimens is to help understand the effect of the interacting variables, such as compressive strength of the grout, wall thickness and diameter of the pipe, diameter of the spliced bars, and the mechanism of mobilizing the confinement action, on the behavior of this type of splice.

Specimens

Four types of single-bar splice specimens were prepared for this experimental study. Lap splice specimens and butt-splice specimens were tested with different confining steel pipe details. Commercially available grouts and pipe were used in all the specimens.

Table 1 shows the properties of the steel pipes used. Fig. 3 provides details of the specimens with further dimensions and properties given in Table 2. Type 1 specimens consist of two lap splices inside a grout-filled pipe (see Fig. 3a). In these specimens, the function of the pipe is to confine the splices only while the load is transferred from one bar, through the confined grout, to the lapping bar and from the lapping bar to the other main bar.

Type 2 specimens are similar to Type 1 specimens with four smaller bars used as lapping bars instead of one equal size bar (see Fig. 3b). The advantages of Type 2 specimens are a smaller diameter steel pipe and a concentric splice. The mechanism of splicing is basically the same as that of Type 1.

Type 3 and 4 specimens are butt splices (see Fig. 3c and 3d, respectively). For these splices to work, the force in one bar is transferred by bond into the grout, from the grout to the pipe, and by the same way to the other bar. In this type of specimen, the bond between the grout and the pipe is very important. Because the pipe is a standard, smooth pipe, bond between its inside surface and the grout is only that due to chemical bond. Unless the compressive stress is significant at the interface between the grout and the pipe, little friction exists between them.

To provide a mechanism that engages the confinement action to increase the transfer-of-force mechanism between the grout and the pipe, for Type 3 specimens a steel ring cut from a smaller pipe diameter is welded to the inside of the pipe on each side, as illustrated in Fig. 3c. The inside diameter of the steel ring is 1.61 in. (40.9 mm). The rings are located 1 in. (25.4 mm) from both ends of the pipe. Steel plates with 1 in. (25.4 mm) diameter holes are welded at both ends of the pipe for Type 4 specimens, as shown in Fig. 3d.

Deformed bars with a minimum yield strength of 60 ksi (414 MPa) were used for the main bars and lapping bars. The specimens were prepared by placing the pipes in a vertical position, with the bars in place, and pouring the grout from the top. The compressive strength of the grouts was measured periodically and on the day of testing using 2 in. (50.8 mm) cubes.

Test Plan and Setup

The specimens were prepared and tested in two stages. The first stage aimed at comparing the various types of splices to obtain an optimum, most practical design, and the second stage aimed at taking a closer look at the behavior of the optimum specimen type. The first stage covered all the specimens except for Type 3, Specimens 4, 5, and 6. These first stage specimens were loaded using a Tinius Olsen testing machine with a load capacity of 120 kips (534.4 kN), as shown in Fig. 4. For these specimens, only the maximum load was measured in addition to observing the failure mode.

Taking into consideration cost and construction flexibility factors, Type 3 specimens were considered the best among all specimens. Thus, Type 3, Specimens 4, 5, and 6 were prepared with a higher strength grout. Specimens 4 and 5 were instrumented with electrical resistance strain gauges at strategic locations to measure longitudinal and tangential (hoop) strains in the pipe as well as axial strains in the bars.

These specimens were tested in displacement control using a closed-loop, servo-operated testing machine (see Fig. 5). The strain changes in the pipe and bars as well as the applied load were recorded using a multi-channel computer-operated data acquisition and reduction system. A calibrated extensiometer was also mounted on one of the main bars for verification of the strain values in the bars.

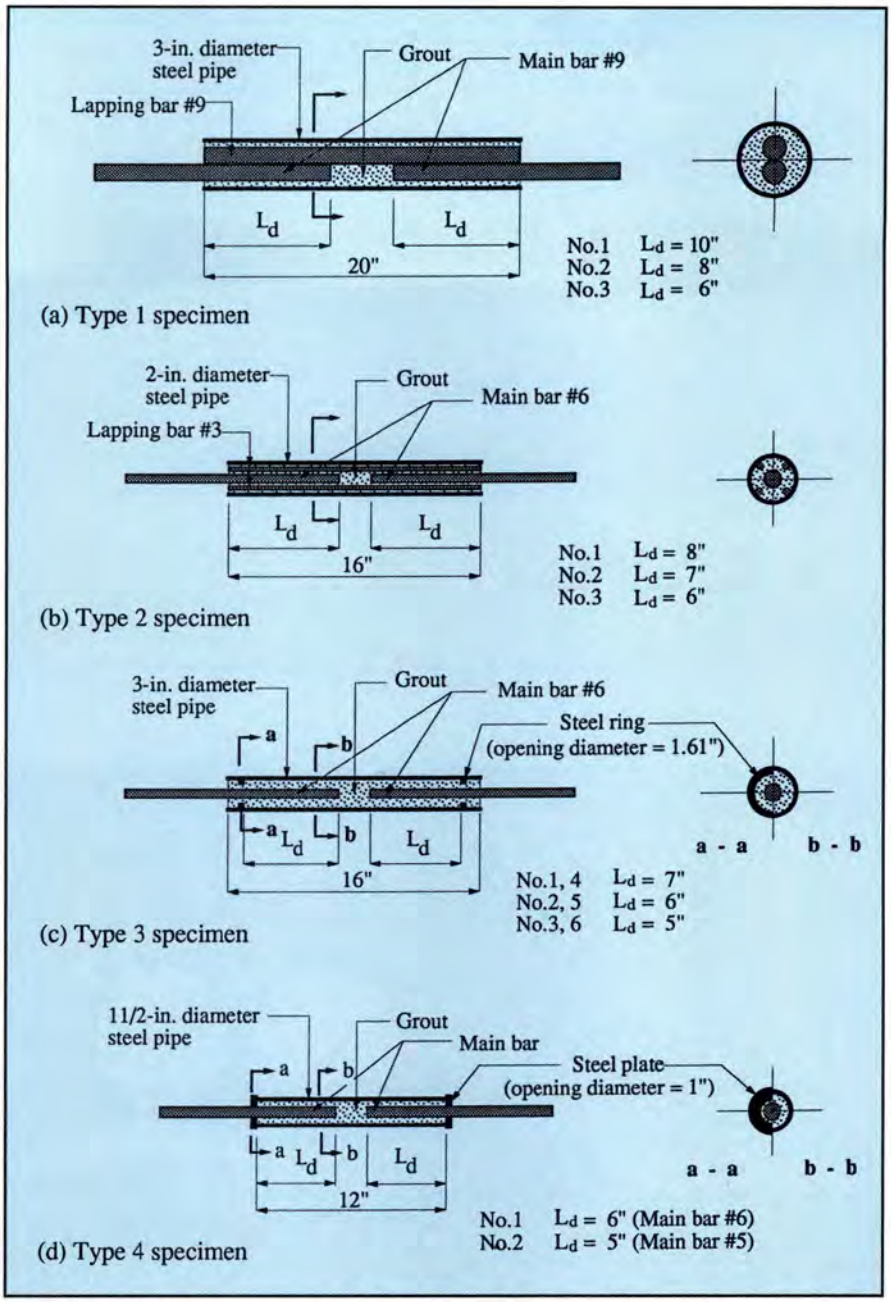

Fig. 3. Details of test specimens. **Note:** 1 in. = 25.4 mm, No. 3 = 10 mm, No. 5 = 16 mm, No. 6 = 19 mm, and No. 9 = 29 mm.

Test Results

The maximum measured axial force was considered the failure load. Table 3 summarizes the test results for all the specimens. When bond failure occurred, the loading was continued to help in determining the failure mechanism. With the exception of Type 3, Specimen 5, all specimens failed in bond, and most specimens failed at an axial stress higher than the yield stress of the bar. Because the high confinement prevents the grout from splitting, the specimens resisted the tensile force until the grout sheared at the outer perimeter of the bar deformations. For Type 3, Specimen 5, the ultimate strength of the bar was reached before bond failure (see Fig. 6).

Type 1 specimens failed in bond where a cylindrical sector of the grout

Table 3. Summary of test results.

Type of specimen	Specimen number	L (in.)	Axial load at failure (kips)	Axial stress at failure (ksi)	Average bond stress (ksi)	Grout compressive strength (ksi)
Type 1 lapping bar	1	10	81.9	81.9	2.30	8.00
	2	8	76.6	76.6	2.70	
	3	6	66.0	66.0	3.10	
Type 2 lapping bar	1	8	40.8	92.7	2.15	6.50
	2	7	30.3	68.9	1.84	
	3	6	26.8	60.9	1.90	
Type 3 steel ring	1	7	35.2	80.0	2.13	6.50
	2	6	25.5	58.0	1.80	
	3	5	23.7	53.9	2.01	
	4	7	45.1	102.5	2.73	10.00
	5	6	44.7	101.6	3.17	
	6	5	33.0	75.0	2.80	
Type 4 steel plate	1	5	30.0	96.8	3.06	6.50
	2	6	44.5	101.1	3.15	

Note: 1 in. = 25.4 mm; 1 ksi = 6.89 MPa; 1 kip = 4.448 kN.

Fig. 5. Test setup for the second stage loading.

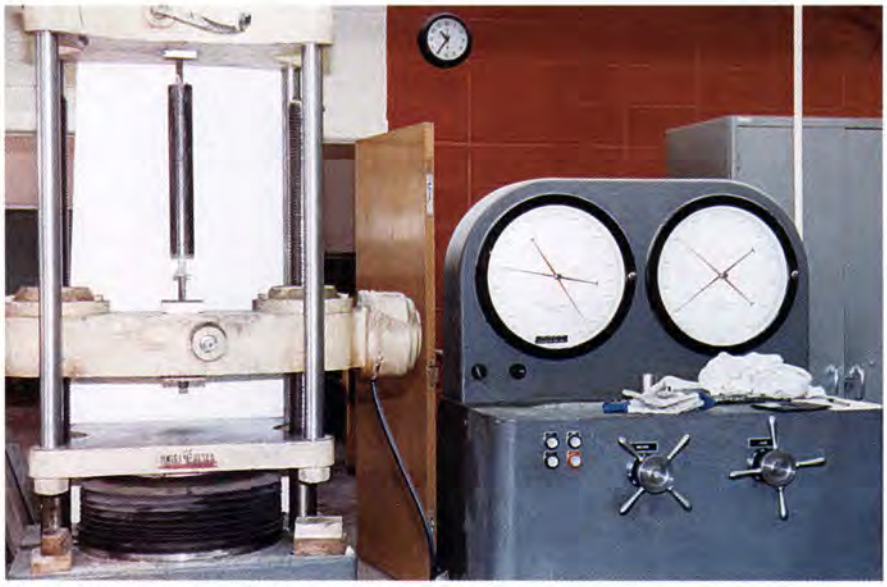

Fig. 4. Test setup for the first stage loading.

split and the load suddenly dropped. Upon further loading, the failed grout sector pulled out of the pipe and was still bonded to the failed main bar (see Fig. 7). The failure surface passed between the failed main bar and the lapping bar and formed an approximate angle of 80 degrees. The interface surface between the failed grout sector and the pipe, when pulled out, appeared clean and smooth, indicating minimal friction or bond to the pipe.

Figs. 8 and 9 show the typical bond failure of Types 2 and 3 specimens, respectively, after the failed main bars were partially pulled out. The clear difference in the amount of grout pulled out with the bar explains the general failure mode of these types of specimens. In Type 2 specimens, the entire amount of grout is held in place by the four lapping No. 3 [10 mm (0.4 in.)] bars inside the sleeve because the total surface area of the lapping bars is greater than that of the main bar; thus, the failure occurred at the perimeter of the main bar.

In Type 3 specimens, however, as the axial load is applied to the main bars, the load transfers to the grout, then from the grout to the pipe, and similarly to the other bar. As observed from the behavior of Type 1 specimens, the load transfer mechanism between the grout and the pipe through chemical bond or friction is relatively weak. However, the rings that are welded to the inside of the pipe from both sides partially prevent the grout from slipping out. This action causes the stress state of the grout to gradually change into a "radial confined splitting" mechanism that gradually increases the compression at the interface between the grout and the pipe resulting in significantly increased friction.

The rings are welded about 1 in. (25.4 mm) from both ends of the pipe to ensure a reliable contact with the grout. The grout portion at the end of the pipe pulls out with the bar because it is not engaged in the confined radial splitting mechanism.

Of the four types, only one specimen was made with two different sizes of bars and embedment lengths, as shown in Fig. 3d and Table 2. Thus, the two different sides of this specimen are considered in Tables 2 and 3 as Type 4, Specimens 1 and 2 and will be referred to thus hereafter. After the failure of Bar 1 in bond, the specimen was placed again in the testing machine, and the load was applied to Bar 2 from one side and to the pipe from the other side. Similarly, Bar 2 failed

Fig. 6. Tensile strength failure, Type 3, Specimen 5.

Fig. 7. Splitting failure, Type 1 specimen.

Fig. 8. Typical bond failure for Type 2 specimens.

Fig. 9. Typical bond failure for Type 3 specimens.

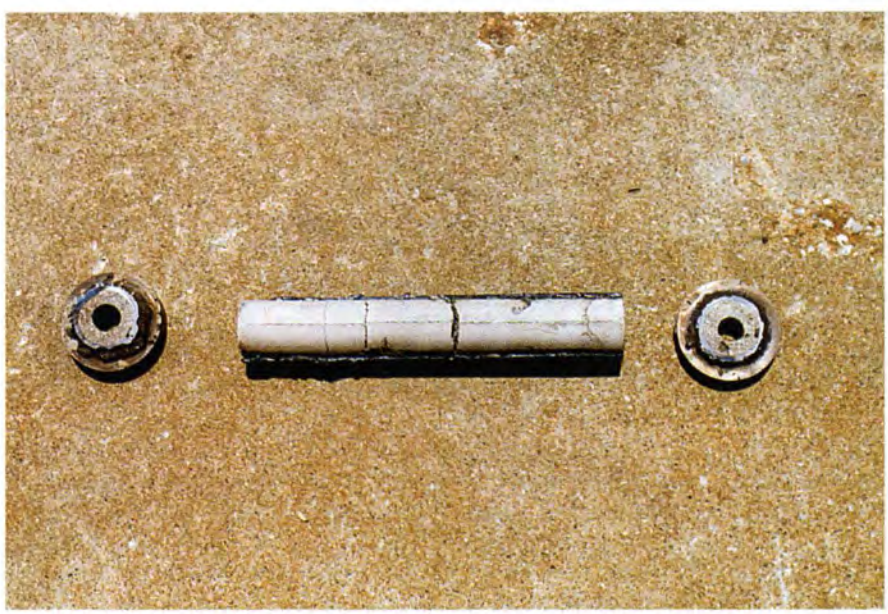

Fig. 10. The grout inside Type 4 specimen.

in bond where the grout sheared at the cylindrical surface passing from the outside edges of the bar deformations.

The pipe was torch-cut to expose the grout and show the failure mode (see Fig. 10). The grout showed a wide crack at mid-length and no crushing at the ends. These signs indicate that as the load was applied to the bars, each bar pulled the surrounding grout with it and the bond between the grout and the pipe broke. It was suspected that small gaps existed between the grout and the end plates that allowed the two broken portions of the grout to move with the bars away from each other and thus develop a wide crack at mid-length. Ultimately, bond failure of both spliced bars governed the capacity of the specimen.

The ultimate capacity of Type 3, Specimens 4, 5, and 6 was at least 125 percent of the specified yield stress of the bars with Specimen 5 reaching ultimate strength of the bar. Figs. 11 and 12 show the locations of strain gauges and the measured strains as functions of applied stress in the main bars, for Specimens 4 and 5, respectively. The gauges were spaced at even spacing, which equals one-third of the effective embedment length of the bar.

Type 4 specimens developed higher average bond strength than Type 2 and 3 specimens with equal grout compressive strength. This could be due to the end plates that completely blocked the motion of the grout, resulting in a high compressive stress at the interface between the plate and the grout. This load transfer mechanism efficiently engages the confinement ac-

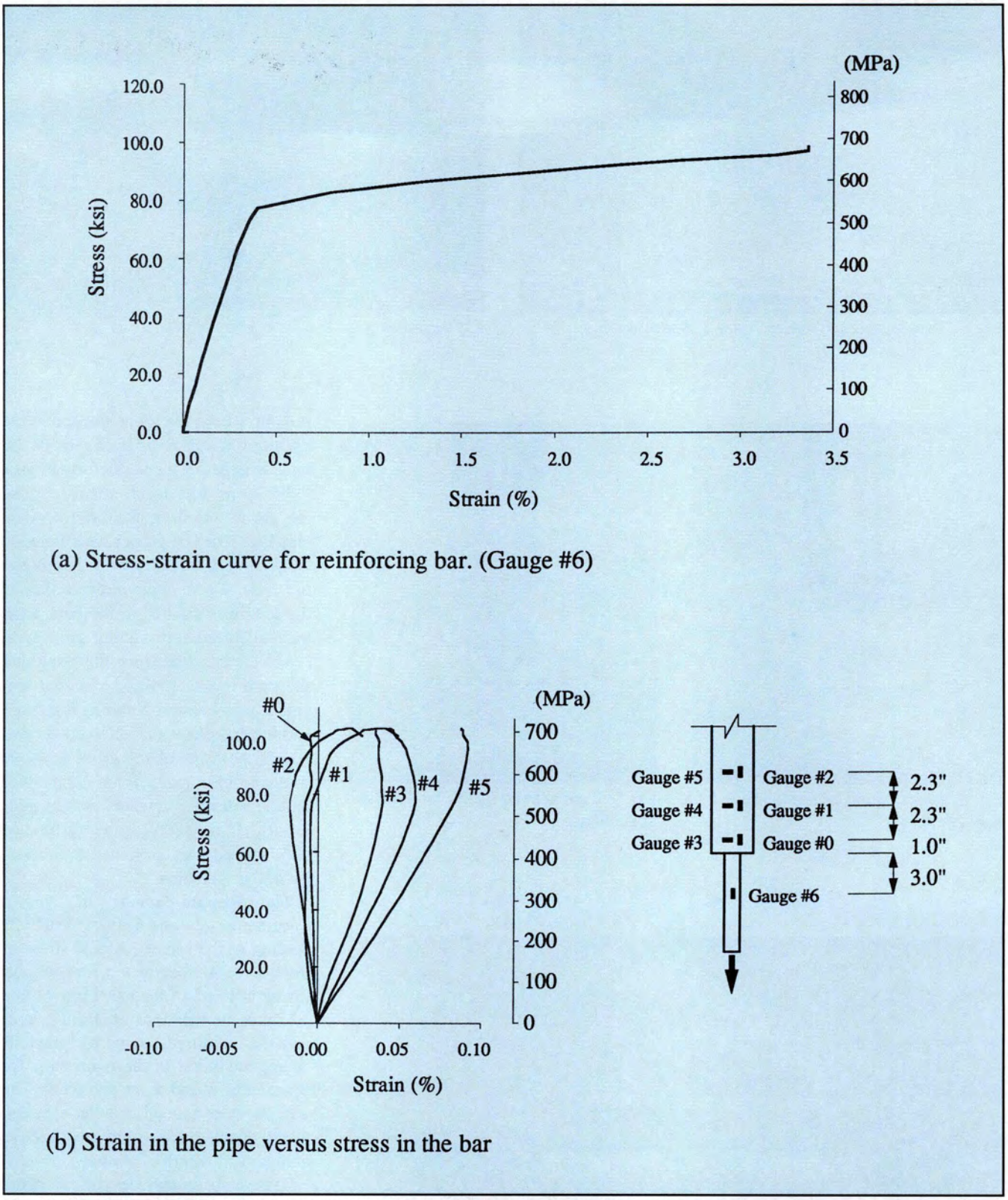

Fig. 11. Stress-strain relationship measured for Type 3, Specimen 4. **Note:** 1 in. = 25.4 mm.

tion to result in high bond strength. Another possible factor is that the stiffness of the end plates in combination with the pipe provided a much more efficient confinement than the pipe did in other specimens.

Splice Type 4 was considered unpractical because it would require tight construction tolerances and would result in initial slip due to air gaps at one or both ends of the splice. Type 1 specimens were also considered impractical because they require larger pipe diameter than other types, extra precaution in detailing and placement due to the eccentricity between the main bars and the pipe, and more materials. Type 2 specimens were also discarded because they provide less room for tolerances than do Type 3 specimens for the same pipe and main bar sizes.

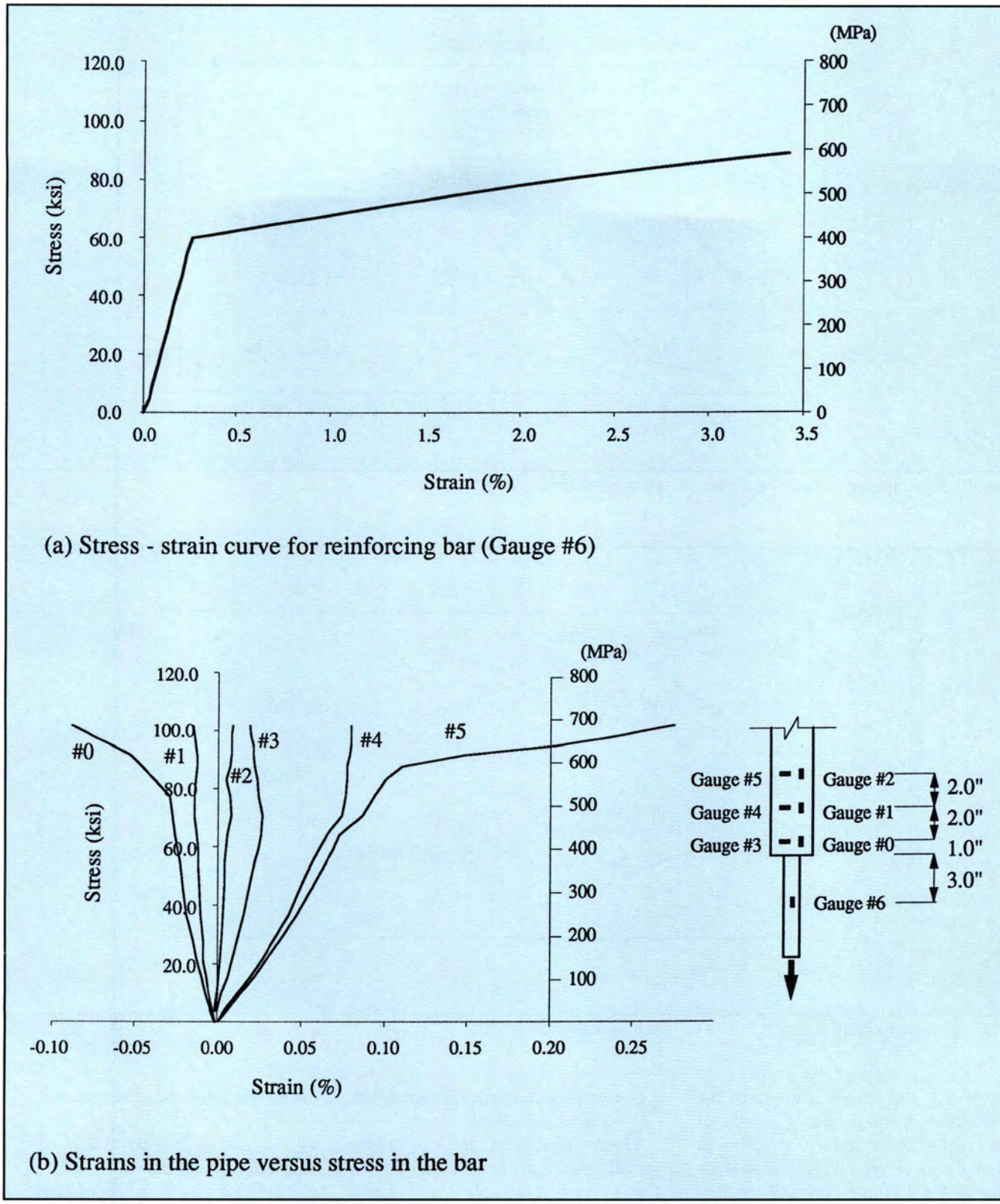

Fig. 12. Stress-strain relationship measured for Type 3, Specimen 5. **Note:** 1 in. = 25.4 mm.

ANALYSIS OF TEST RESULTS

The variables that may affect the bond strength of reinforcing bars confined with steel pipe include the yield strength of the reinforcing bar, the grout strength, the properties of the pipe, and the geometry of the bar and its confining region. Geometrical variables include the bar diameter and its embedment length into the confined grout, the inside diameter of the pipe, the pipe's wall thickness, and the geometry of the pipe's free ends. The following analysis aims to study the test results in light of existing bond strength theory.

Axial stress in the bar at failure is listed in Table 3 and plotted in Fig. 13 as a function of lap or embedment

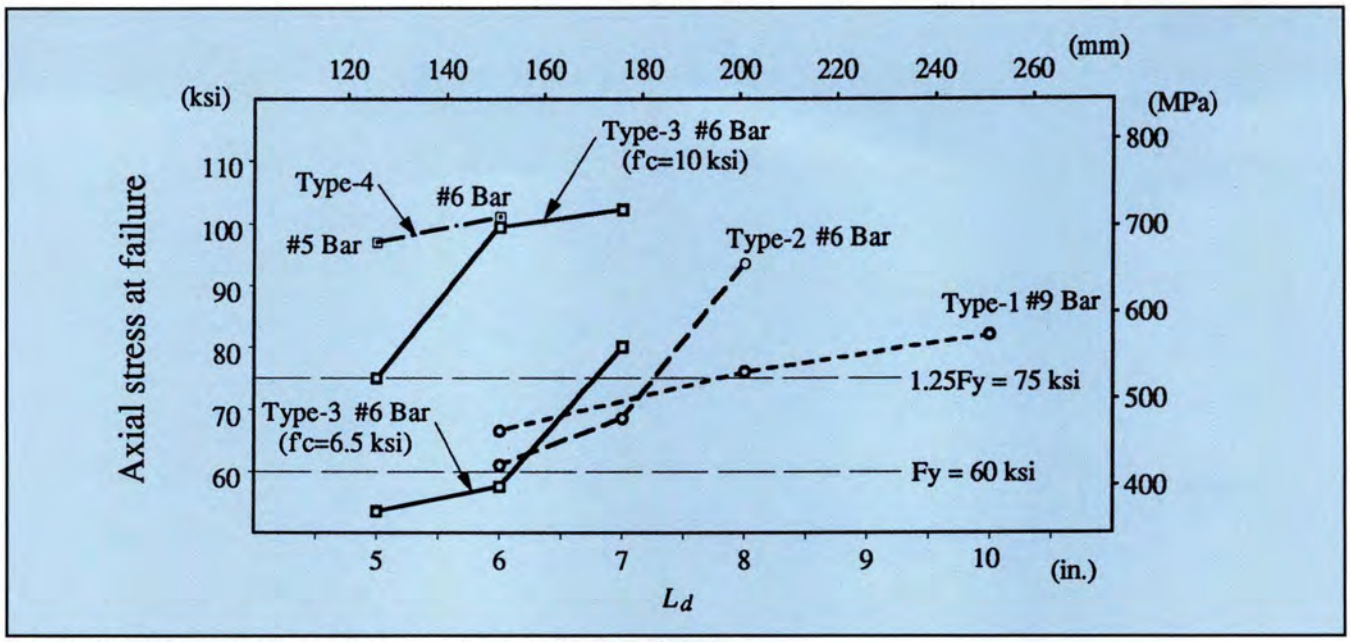

Fig. 13. Axial stresses in the main bars vs. lap or embedment length.

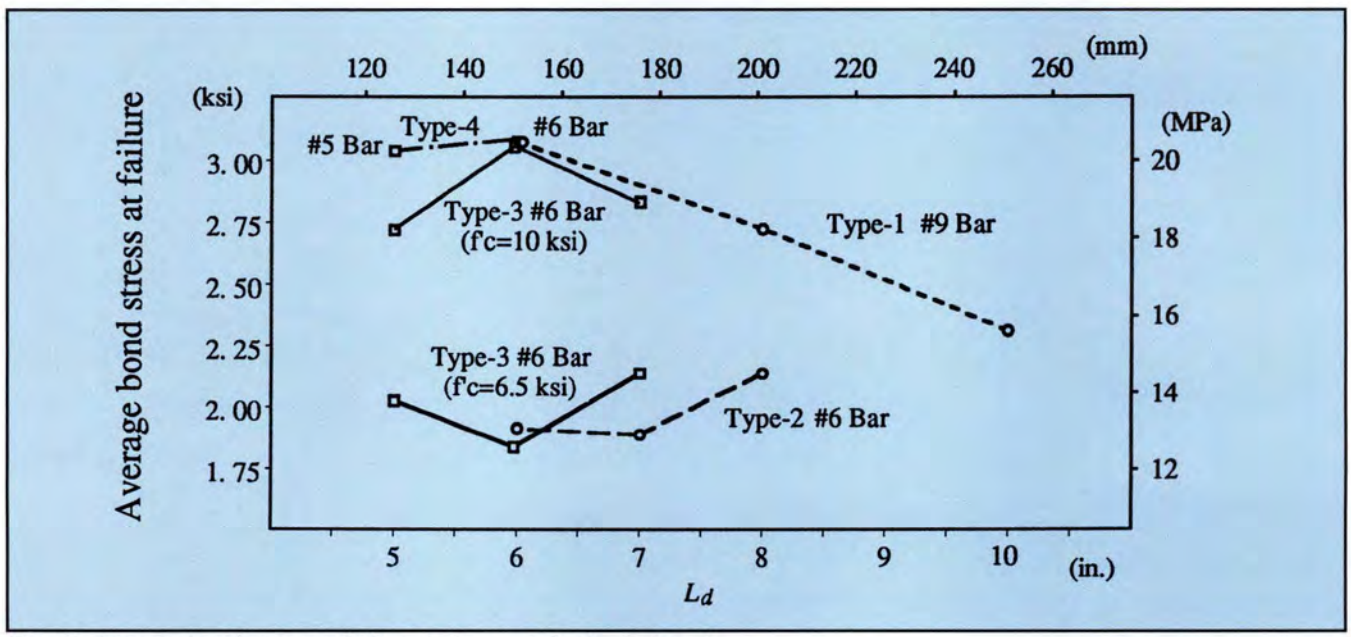

Fig. 14. Average bond stress at failure vs. lap or embedment length.

length L_d. The tensile strength of the tested specimens increases as a function of L_d and the grout's compressive strength for all types of specimens. Although bond failure occurs at the outside surface of the bar deformations, average bond stress at failure, U, is calculated below using the nominal bar diameter, as follows:

$$U = \frac{P}{\pi D L_d} \quad (1)$$

where

P = failure load

D = nominal diameter of the main bar

L_d = lap or embedment length

The average bond stress at failure for all specimens as calculated from Eq. (1) is listed in Table 3, and plotted as a function of L_d in Fig. 14. As the figure shows, there is a clear indication that the bond stress at failure increases with f'_c (compressive strength of the grout). Fig. 15 shows the relationship between L_d and $U/\sqrt{f'_c}$. It can be seen that the variation of the quantity $U/\sqrt{f'_c}$ as a function of L_d is minimal for each type of specimen. Thus, a linear relationship can be assumed:

$$U = k\sqrt{f'_c} \quad (2)$$

where k is a constant.

The approximate values of k are 30, 25, 27, and 38 for Types 1, 2, 3, and 4, respectively.

The measured load and strain values obtained from testing Type 3, Specimens 4 and 5 deserve special attention. The measured axial and tangential strains in the sleeve remained linear until the bar started yielding. Note that the actual yielding stress of

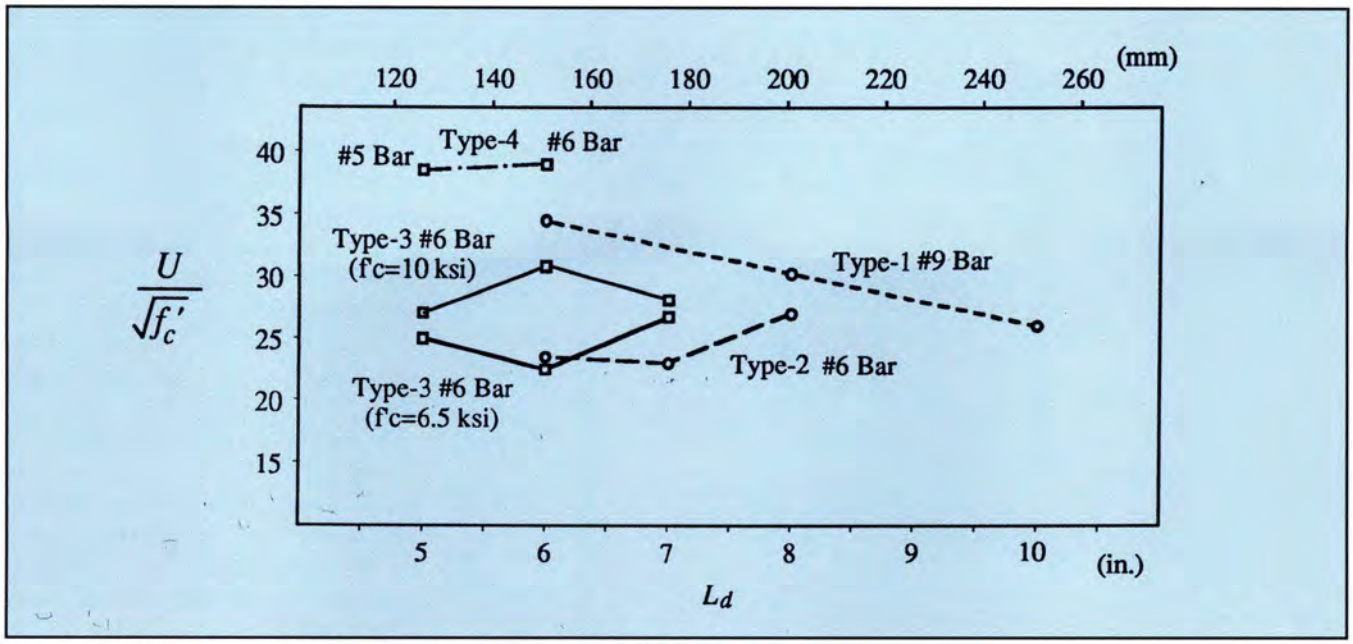

Fig. 15. Relationship between $U/\sqrt{f_c'}$ and lap or embedment length.

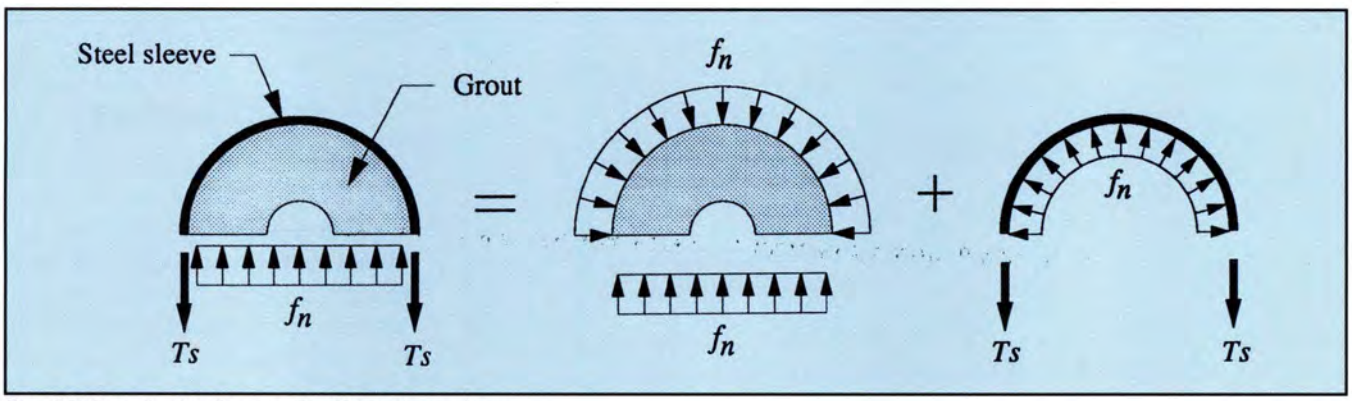

Fig. 16. Free body diagram for Type 3 specimen.

the bar is 62 ksi (427 MPa) as obtained from a single bar test. When the bar starts yielding, at the entrance to the grout or outside the sleeve where the stress is the highest, the strain in the sleeve started to drop in Specimen 4 where bond failure occurred. The strain then remained constant or increased in Specimen 5 where ultimate strength of the bar occurred, as shown in Figs. 11 and 12, respectively.

Gauge 5 of Specimen 5 indicates yielding of the pipe in the tangential direction. The actual yield stress of the pipe as measured from a material test is 33.5 ksi (231 MPa). Tangential yielding of the pipe would result in a reduction of confinement that may in turn lead to bond failure.

As indicated above, the main bar of Type 3, Specimen 5, failed as it reached its ultimate strength after some of the grout chipped, as shown in Fig. 3. The bar broke at the location of Gauge 6. The ultimate strength of the bar in this specimen was slightly lower than the bond strength of Specimen 4, although its embedment length in Specimen 5 was shorter than that in Specimen 4. The actual ultimate strength of the bar as tested separately without grinding damage is 101.7 ksi (701 MPa). Excessive grinding of the bar for mounting Gauge 6 of Specimen 5 was suspected as the reason for its ultimate strength failure at this stress level.

A complicated stress state exists in the embedment length region of the splice. The axial stress in the pipe is expected to increase from zero at the ends to a maximum at the end of the bar near mid-length of the pipe. The strain gauges that are oriented to measure the axial strain in the pipe, Gauges 0, 1, and 2, indicated linearly increasing compression strain rather than the expected tension. At this stage, the main bar started yielding and the measured strain values started changing direction rapidly until failure, where Gauges 1 and 2 were measuring positive strain. This strain state can be attributed to Poisson's effect, which may be significant in such a complicated and intense stress state in the pipe.

Untrauer and Henry[1] derived the following equation to describe the bond strength of concrete U as a function of its compressive strength f_c' and lateral confining pressure f_n:

$$U = \left(18 + 0.45\sqrt{f_n}\right)\sqrt{f_c'} \qquad (3)$$

Using the free body diagram shown

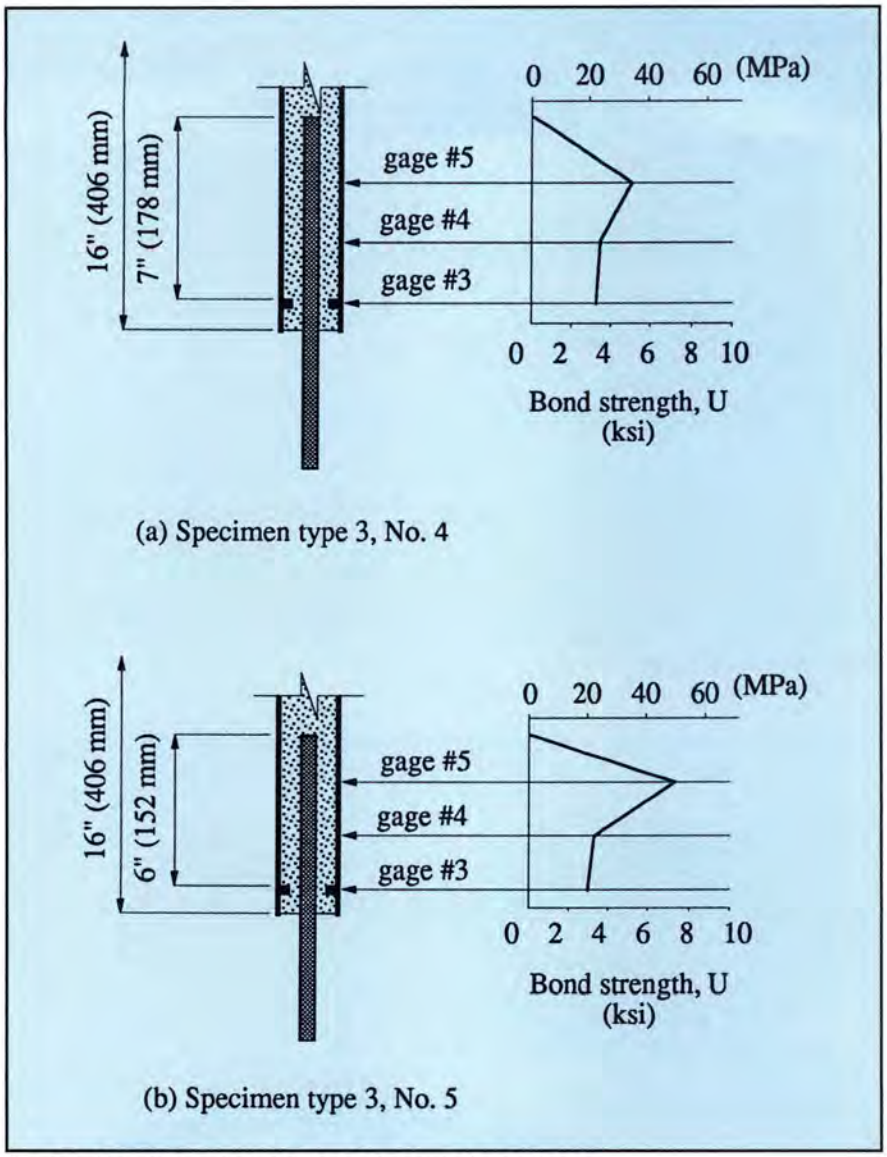

Fig. 17. Calculated ultimate bond strength of specimens.

in Fig. 16, confining pressure can be calculated from measured tangential strain in the pipe, as follows:

$$T_s = \varepsilon_s t(\Delta l)E \quad (4)$$

$$f_n = \frac{2T_s}{d_i(\Delta l)} = \frac{2\varepsilon_s t(\Delta l)E}{d_i(\Delta l)} = \frac{2\varepsilon_s tE}{d_i} \quad (5)$$

where

T_s = tangential (hoop) force in a small length Δl of the pipe
ε_s = tangential strain in the pipe
t = thickness of pipe wall
Δl = small longitudinal length of the pipe
E = modulus of elasticity of the pipe
d_i = inside diameter of the pipe

From Eqs. (3) and (5), assuming that the pipe yields when ultimate bond strength is reached, it can be seen that as the inside diameter of the pipe increases without changing its wall thickness, confining pressure decreases. Therefore, ultimate bond stress decreases, and hence, splice capacity decreases. It can also be inferred that as the wall thickness of the pipe increases without changing its inside diameter, confining pressure increases. Therefore, ultimate bond stress increases and, hence, the splice capacity increases.

Ultimate bond stress at failure, U, as calculated from the measured tangential strain values in the pipe, is shown in Fig. 17. The ultimate bond strength of the specimen can thus be calculated as the area of the ultimate bond stress diagram times the circumference of the bar.

The calculated bond strengths of Specimens 4 and 5 using this method are 57 and 61 kips (250 and 271 kN), respectively. These calculated values of the ultimate bond strength are different from the measured capacities for the following reasons:

1. The available limited resources for this test program did not allow more elaborate and comprehensive instrumentation of the specimens; thus, the available test results allowed only a rough estimation.

2. The radial strains that are measured and used in the calculation do not accurately represent the actual radial stress; only specially designed rosettes can provide enough data to accurately measure the full strain field in this case.

3. Specimen 5 failed in ultimate strength of the bar as mentioned earlier, and thus its actual ultimate bond strength is unknown.

CONCLUSIONS

The results of this experimental program provide valuable data on the effect of grout compressive strength and level of confinement on the bond strength of reinforcing bars. More importantly, it shows that a simple, nonproprietary, and inexpensive grout-filled splice for field connection of precast concrete members can be fabricated from standard steel pipe. The investigation focused on a simple splice detail that is capable of developing a minimum strength of 125 percent of the bar's specified yield strength with the potential to develop the ultimate strength of the bar. In addition, the following particular conclusions can be made:

1. High bond strength of reinforcing bars can be achieved by confining the grout surrounding the bars. Lap splice or embedment lengths as short as seven times the bar diameter can achieve bar development when the appropriate grout compressive strength and confinement are provided.

2. With grout-filled butt pipe splices, a high splicing strength can be obtained by welding steel rings on the inside of the pipe at both ends. A small reduction in the pipe end opening is sufficient to mobilize the grout

confining action that results in high bond strength.

3. More extensive testing with various grout compressive strengths and pipe geometry variations needs to be conducted in order to generate design tables or other design aids for this type of splice for various bar sizes.

4. The experiments and analysis presented are based on static loads only and without measuring the possible slippage of the spliced bars. Unless the slippage of the bars due to axial load in this type of splice is adequately investigated, this splice should not be used in construction of actual structures. In addition, unless the behavior of this splice is proven adequate for cyclic and fatigue loading, the splice should not be used in structures subject to cyclic or fatigue loads.

ACKNOWLEDGMENT

The authors acknowledge the financial support of the Center for Infrastructure Research, University of Nebraska-Lincoln, and the Civil Engineering Department at the University of Nebraska at Omaha. The donation of steel pipe by Paxton and Vierling Steel Company, Omaha, Nebraska, and the donation of reinforcing bars by Wilson Concrete Company, Bellevue, Nebraska, are appreciated.

REFERENCES

1. Untrauer, R. E., and Henry, R. L., "Influence of Normal Pressure on Bond Strength," *ACI Journal,* V. 62, No. 5, May 1965, pp. 577-585.
2. Nilson, A. H., "Internal Measurement of Bond Slip," *ACI Journal,* V. 69, No. 7, July 1972, pp. 439-441.
3. Losberg, A., and Olssen, P., "Bond Failure of Deformed Main Bars Based on the Longitudinal Splitting Effect of the Bars," *ACI Journal,* V. 76, No. 1, January 1979, pp. 5-18.
4. Yankelevsky, D. Z., "Bond Action Between Concrete and a Deformed Bar — A New Model," *ACI Journal,* V. 82, No. 2, March-April 1985, pp. 154-162.
5. Soroushian, P., and Choi, K., "Local Bond of Deformed Bars with Different Diameters in Confined Concrete," *ACI Structural Journal,* V. 86, No. 2, March-April 1989, pp. 217-222.
6. Soroushian, P., Choi, K., Park, G., and Aslani, F., "Bond of Deformed Bars to Concrete: Effects of Confinement and Strength of Concrete," *ACI Materials Journal,* V. 88, No. 3, May-June 1991, pp. 227-232.
7. Hayashi, Y., Shimizu, R., Nakatsuka, T., and Suzuki, K., "Bond Stress-Slip Characteristic of Reinforcing Bar in Grout-Filled Coupling Steel Sleeve," *Proceedings,* Japan Concrete Institute, V. 15, No. 2, 1993, pp. 265-270.
8. Nomura, K., Hara, N., Mutsuyoshi, H., and Machida, A., "Experimental Study on Joints of Main Bars in Prestressed Concrete Formworks," *Proceedings,* Japan Concrete Institute, V. 15, No. 2, 1993, pp. 259-264.
9. Adajar, J., Yamaguchi, T., and Imai, H., "An Experimental Study on the Tensile Capacity of Vertical Bar Joints in a Precast Shearwall," *Proceedings,* Japan Concrete Institute, V. 15, No. 2, 1993, pp. 1255-1261.